Some Finite Elements Having Particular Application to Box Girder Bridges

Quelques éléments finis d'application particulière
aux ponts à poutres en caisson

Finite Elemente für die Berechnung von Brücken
mit Kastenquerschnitt

K. R. MOFFATT
Imperial College of Science and Technology also
Structures and Computers Ltd, London, England

P. T. K. LIM
Structures and Computers Ltd,
London, England

SUMMARY

Details are given of several new finite elements which are especially suitable for use in the analysis of box girder bridges. Results of three model tests are used as a basis for demonstrating the accuracy of the elements. Recommendations are made on the element type and size necessary for the economic and accurate analysis of box girder bridges.

RÉSUMÉ

Les auteurs présentent en détail plusieurs nouveaux éléments finis particulièrement utiles dans le calcul de ponts à poutres en caisson. Les résultats de trois essais sur modèle prouvent la précision de ces éléments. Des recommandations sont faites quant au type d'élément et à sa dimension nécessaire pour un calcul économique et précis de ponts à poutres en caisson.

ZUSAMMENFASSUNG

Es wird über einige neue finite Elemente berichtet, welche bei der Berechnung von Brücken mit Kastenquerschnitt besondere Vorteile bieten. Die Resultate von drei Testbeispielen erlauben die Beurteilung der erreichbaren Genauigkeit. Empfehlungen für die Wahl von Elementtyp und -grösse im Hinblick auf eine rasche und genaue Berechnung von Brücken mit Kastenquerschnitt beschliessen den Aufsatz.

1. INTRODUCTION

Early finite element analyses of box girder bridges [1,2] employed the basic
rectangular extensional-flexural element, the stiffness matrix of which is
formed from the stiffness matrices of the basic extensional and flexural
elements [3]. This rectangular extensional-flexural element is a special case
of the more general quadrilateral element Q23* which has at each of its four
nodal points two in-plane degrees of freedom u and v and three out-of-plane
degrees of freedom w, θ_x, and θ_y, but no in-plane rotational degree of freedom
θ_z (Fig. 1). A large number of these elements must be used in the analysis of
a box girder bridge since the element is not well suited to representing the
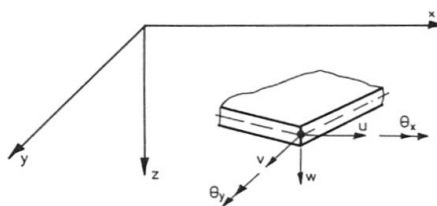predominate in-plane bending action of the webs.

Fig.1 Nodal degrees of freedom associated with
basic extensional-flexural element

Lim et al. [4] and Sisodiya et al. [5] have achieved more economical solutions
by using a quadrilateral extensional-flexural element Q33, the stiffness matrix
of which is formed from the stiffness matrices of a higher order extensional
element Q30 and the basic flexural element Q03. This particular extensional-
flexural element has a bias, beam-type, in-plane displacement field by virtue
of the presence of a further in-plane degree of freedom $\partial v/\partial x$ at each node in
place of the 'free' in-plane rotation θ_z. This displacement field can closely
approximate the deformation of the webs of a box girder bridge and the overall
behaviour of the bridge can therefore be obtained with the use of a relatively
coarse mesh division. However, as in the case of the element Q23, this element
has the disadvantage that the in-plane longitudinal strain cannot vary over the
length of the element. Consequently, an accurate estimation of the local
stresses in the region of an intermediate support or a wheel load would require
the use of a localized fine mesh division and an extrapolation procedure.

The question arises, therefore, as to whether more economical solutions could
be obtained by using elements having higher order displacement functions. The
specification of higher order displacement functions requires the introduction
of either additional nodal degrees of freedom or additional side nodes. In
general, for the same order of displacement functions, the introduction of
additional nodal degrees of freedom rather than additional side nodes results
in a smaller number of unknowns and a smaller bandwidth in the stiffness matrix
of the overall structure. These observations led the Writers to develop a
higher order quadrilateral element Q43, which has a further nodal 'degree of
freedom' $\partial u/\partial x$ chosen to permit a variation of the in-plane longitudinal strain
over the length of the element. A description of this element is given in this
paper.

---

*The elements referred to in this paper have been given an 'alpha-numeric'
name, the alphabetic component of which indicates the shape of element (Q for
quadrilateral and T for triangle), and the numeric component of which indicates
the number of degrees of freedom at each node (first numeral for extensional
degrees of freedom and second numeral for flexural degrees of freedom).

In the idealization of skewed bridges, it is often convenient to use rectang-
ular elements and to adjust the mesh to the skewed boundaries using triangular
elements. Also, studies have shown that for a given number of nodes more
accurate results are obtained when rectangular and triangular elements are
used instead of parallelogrammic elements to idealize a skewed region [6].
For these reasons, two triangular elements T33 and T43, that are suitable for
use with the elements Q33 and Q43, respectively, are also presented in this
paper.

In parallel with the development of new elements, there is a need for compara-
tive studies of the effect of element type and size on accuracy in order that
recommendations may be made on the use of such elements. Some results of such
a study are noted in this paper.

2. DESCRIPTION OF ELEMENTS

This section describes a quadrilateral extensional element Q40, and two triang-
ular extensional elements T30 and T40. The stiffness matrices for the extens-
ional-flexural elements Q43, T33, and T43 are formed from those of the elements
Q40, T30, and T40, respectively, and from that of the basic quadrilateral flex-
ural element Q03 [7] or the basic triangular flexural element T03 [3], as
appropriate.

2.1 Quadrilateral Element Q40

The element Q40 has four nodes, each of which has four degrees of freedom u, v,
$\partial v/\partial x$, and $\partial u/\partial x$, where u and v are translations parallel to the x and y axes
of the element, respectively. Such a choice of nodal degrees of freedom
enables the element displacement functions to be specified as follows:

$$u = \alpha_1 + \alpha_2\xi + \alpha_3\eta + \alpha_4\xi^2 + \alpha_5\xi\eta + \alpha_6\xi^3 + \alpha_7\xi^2\eta + \alpha_8\xi^3\eta$$

$$v = \alpha_9 + \alpha_{10}\xi + \alpha_{11}\eta + \alpha_{12}\xi^2 + \alpha_{13}\xi\eta + \alpha_{14}\xi^3 + \alpha_{15}\xi^2\eta + \alpha_{16}\xi^3\eta$$

where ξ and η are the generalized co-ordinates of the element (Fig. 2), and α_1
to α_{16} are arbitrary coefficients. These displacement functions satisfy the
compatibility condition for continuous displacement between adjacent elements
and the constant strain criterion for rectangular, parallelogrammic, and
trapezoidal elements but not for a general quadrilateral element. (A similar
comment can be made in respect of the displacement functions for the element
Q30. However, Sisodiya et al. [5] have shown that good results can be obtained
when the element Q30 is used as a general quadrilateral.) The formulation of
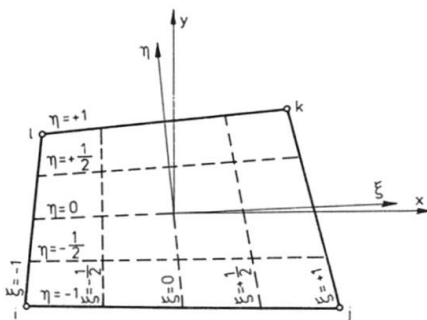

Fig.2 Quadrilateral element and generalized
co-ordinate system

the element stiffness and stress matrices follows the same procedure as that described in Ref. 7 and therefore will not be described here.

The following points refer to the use of the element Q40:
(a) Each element should be oriented such that its x-axis is in a direction parallel to the direction of the predominant bending stresses in the structure.
(b) In the assembly of the stiffness matrix of the overall structure, the element stiffness terms corresponding to the strain component $\partial u/\partial x$ should be treated as local degrees of freedom for which no transformation to the global co-ordinate system is necessary.
(c) The element should strictly not be used in cases where an abrupt change of material rigidity gives rise to a discontinuity in the strain component $\partial u/\partial x$ in the x-direction. However, it is shown in Ref. 8 that, in most practical cases of such an abrupt change, good results can be obtained with the element.

2.2 Triangular Element T30

The element T30 has three degrees of freedom u, v, and $\partial v/\partial x$ at each of its three nodes and has the following displacement functions:

$$u = \alpha_1 + \alpha_2 x + \alpha_3 y$$

$$v = \alpha_4 + \alpha_5 x + \alpha_6 y + \alpha_7 x^2 + \alpha_8 xy + \alpha_9 x^3$$

These displacement functions satisfy the constant strain criterion, while the compatibility condition for continuous displacement between this element and the element Q30 will be satisfied when the elements are assembled as shown in Fig. 3. The element stiffness and stress matrices can be obtained using the procedures given in Ref. 4, and will not be derived here.
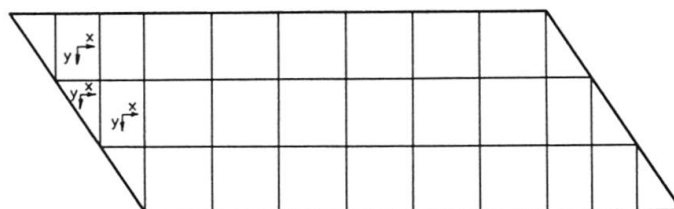
Fig.3   Discretization of a skewed region using
triangular and rectangular elements

2.3 Triangular Element T40

The element T40 has four degrees of freedom u, v, $\partial v/\partial x$, and $\partial u/\partial x$ at each of its three nodes and has the following displacement functions:

$$u = \alpha_1 + \alpha_2 x + \alpha_3 y + \alpha_4 x^2 + \alpha_5 xy + \alpha_6 x^3$$

$$v = \alpha_7 + \alpha_8 x + \alpha_9 y + \alpha_{10} x^2 + \alpha_{11} xy + \alpha_{12} x^3$$

These displacement functions satisfy the constant strain criterion, while the compatibility condition for continuous displacement between this element and the element Q40 will be satisfied when the elements are assembled as shown in Fig. 3. Again, the procedures given in Ref. 4 can be used to obtain the element stiffness and stress matrices.

3. APPLICATIONS

In an earlier study [9], the elements Q23, Q33, Q43, T33, and T43 were used in the analysis of several right and skewed single cell box girders, for which theoretical solutions were available. Some findings of the study are summarized here: (a) the accuracy of the results obtainable using the element Q23 deteriorates rapidly as the aspect ratio (length/depth) of the web elements increases above unity; (b) the accuracy of the results obtainable using the element Q33 or the element Q43 is relatively independent of the element aspect ratio, and reliable results are obtainable with as few as six and four mesh divisions, respectively, along each span and with one mesh division over the depth of each web; and (c) for a given number of degrees of freedom, more accurate results are obtained when skewed girders are analysed using a combination of the elements T33 and Q33 or of the elements T43 and Q43 than when the element Q33 or the element Q43 is used exclusively.

To highlight some of the above points, reference is now made to the analysis of three box girder bridge models.

3.1 Straight Three Cell Box Girder Bridge Model

Figure 4 shows the details of a straight three cell box girder bridge model

Fig. 4 Straight three cell box girder bridge model.
Details of model and loading

which was analysed using the elements Q23, Q33, and Q43. The model, a 1/60th
scale representation of an approach span to the Lower Yarra Bridge, Melbourne,
Australia, was made of perspex. The results presented here are for a load
placed eccentrically on the model by means of a cantilever at the mid-span
(Fig. 4).

Owing to symmetry, only one half of the model was analysed with the finite
element discretizations shown in Fig. 5. Two of the solutions were obtained
using the element Q23 or the element Q33 throughout, while the third solution
was obtained using the element Q43 for the webs and flanges and the element Q33
for the diaphragms*. In each case, the support stiffnesses were transformed to
the nodes at the outer webs assuming the diaphragms to be infinitely rigid in
their own plane. The idealizations were selected so that the various analyses
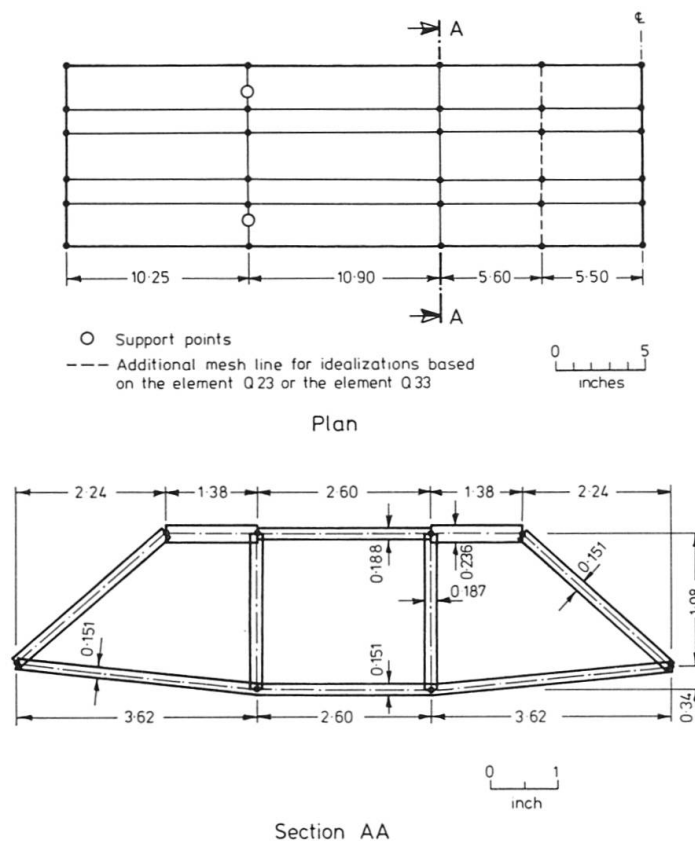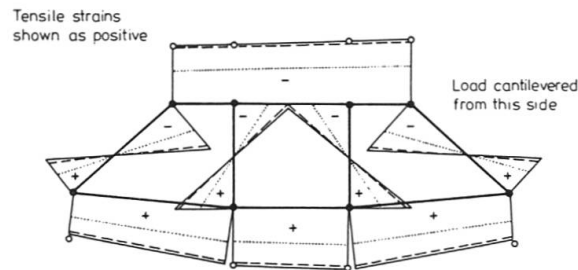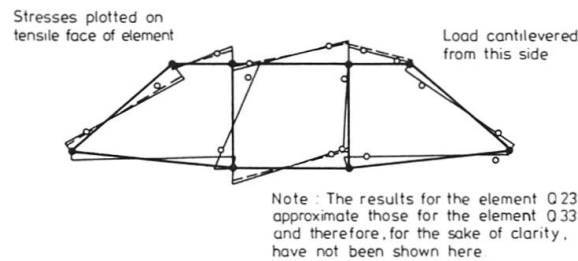involved approximately the same computer cost.

Fig.5   Straight three cell box girder bridge model.
Finite element idealizations

---

*Since only one local degree of freedom corresponding to the strain component
∂u/∂x was considered in the stiffness matrix of the overall structure, it was
necessary to use the element Q33 for representing the diaphragms.

Some comparisons between the finite element and experimental values of stress
are given in Fig. 6. It can be seen that the results are in good agreement,
except for those obtained using the element Q23.

Tensile strains
shown as positive

Load cantilevered
from this side

(a) Distribution of longitudinal outer surface strains

Stresses plotted on
tensile face of element

Load cantilevered
from this side

Note : The results for the element Q 23
approximate those for the element Q 33
and therefore, for the sake of clarity,
have not been shown here

(b) Distribution of transverse flexural strains

.... Solution using element Q 23

－ － － － Solution using element Q 33

────── Solution using element Q 43

o   Experimental values

0   200
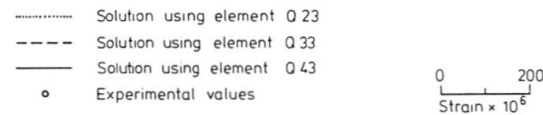Strain × 10⁶

Fig. 6 Straight three cell box girder bridge model.
        Distribution of strains at section 5·5in from
        mid-span for model under eccentric point
        load at mid-span

3.2 Curved Single Cell Box Girder Bridge Model

Figure 7 shows the details of a curved single cell box girder bridge model
which was analysed using the elements Q23, Q33, and Q43. The model, a 1/30th
scale representation of a proposed slip-road structure for the Stockton Road
Interchange at Teesside, England, was made of an araldite and sand mixture.

Owing to symmetry, only one half of the model was analysed with the finite
element discretizations shown in Fig. 8. Two of the solutions were obtained
using the element Q23 or the element Q33 throughout, while the third solution
was obtained using the element Q43 for the webs and flanges and the element Q33
for the diaphragms. Again, the three analyses involved approximately the same
computer cost.

Some finite element and experimental values of stress obtained for a point load
of 100 lbf placed over the outer web at the mid-span are given in Fig. 9. It
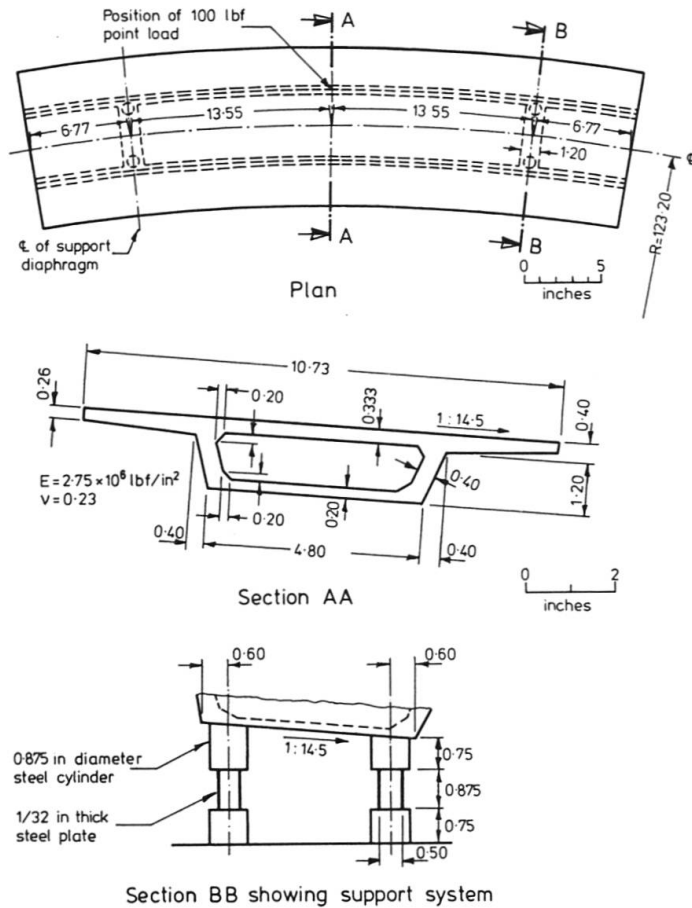can be seen that, except for the values pertaining to the element Q23, the

Fig. 7   Curved single cell box girder bridge model.
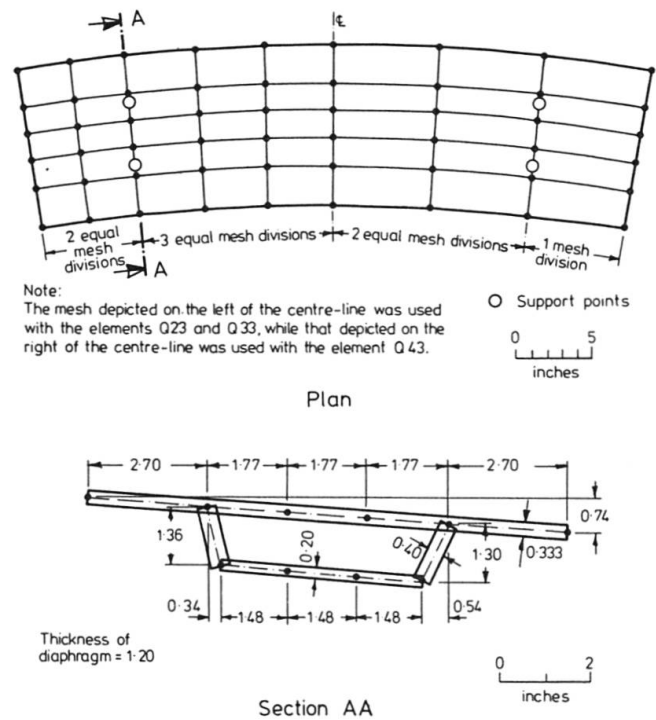Details of model and loading

Fig. 8   Curved single cell box girder bridge model.
Finite element idealizations.

finite element and experimental results are in close agreement. It should be
noted, however, that in the case of the elements Q23 and Q33 it was necessary
to use an extrapolation procedure in order to obtain the results shown, whereas
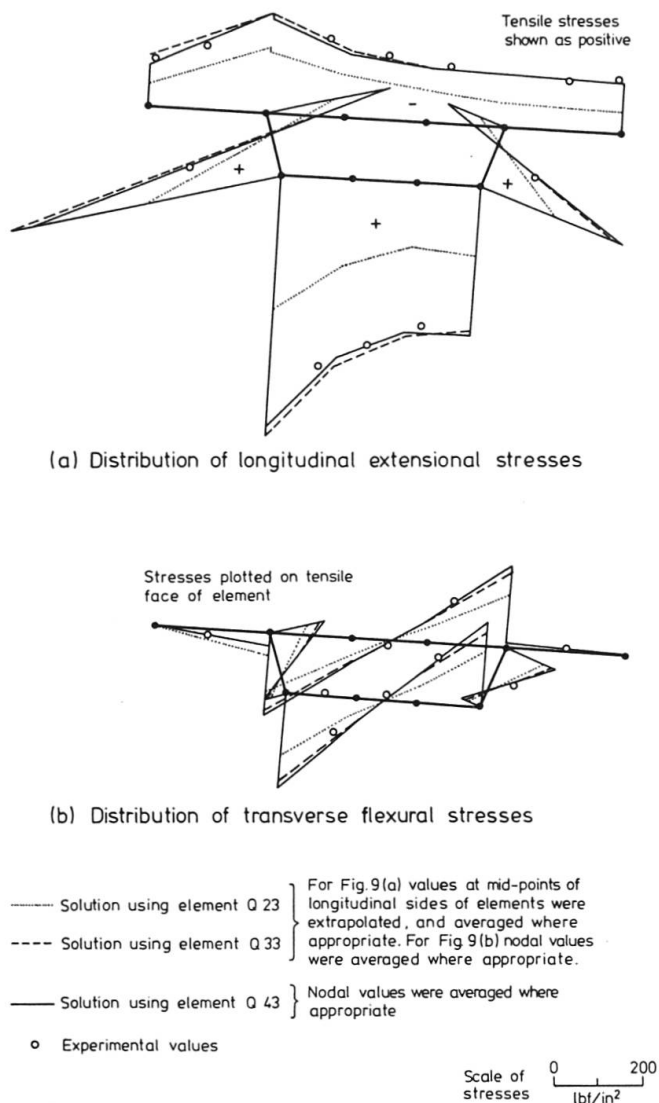in the case of the element Q43 the results were obtained directly.

(a) Distribution of longitudinal extensional stresses

(b) Distribution of transverse flexural stresses

Fig. 9   Curved single cell box girder bridge model.
          Distribution of stresses at centre cross-
          section for model under eccentric point
          load at mid-span

3.3 Skewed Composite Twin Cell Box Girder Bridge Model

Figure 10 shows the details of a skewed composite twin cell box girder bridge
model [10]; the deck and diaphragms were made of an araldite and sand mixture,
while the boxes were formed from a mild steel sheet. The load case considered
here is also shown in Fig. 10. The model was analysed using a combination of
the elements T33 and Q33 with the finite element discretization shown in
Fig. 11.

Some comparisons between the finite element and experimental values of stress
are given in Fig. 12. It can be seen that these results are in close agreement.
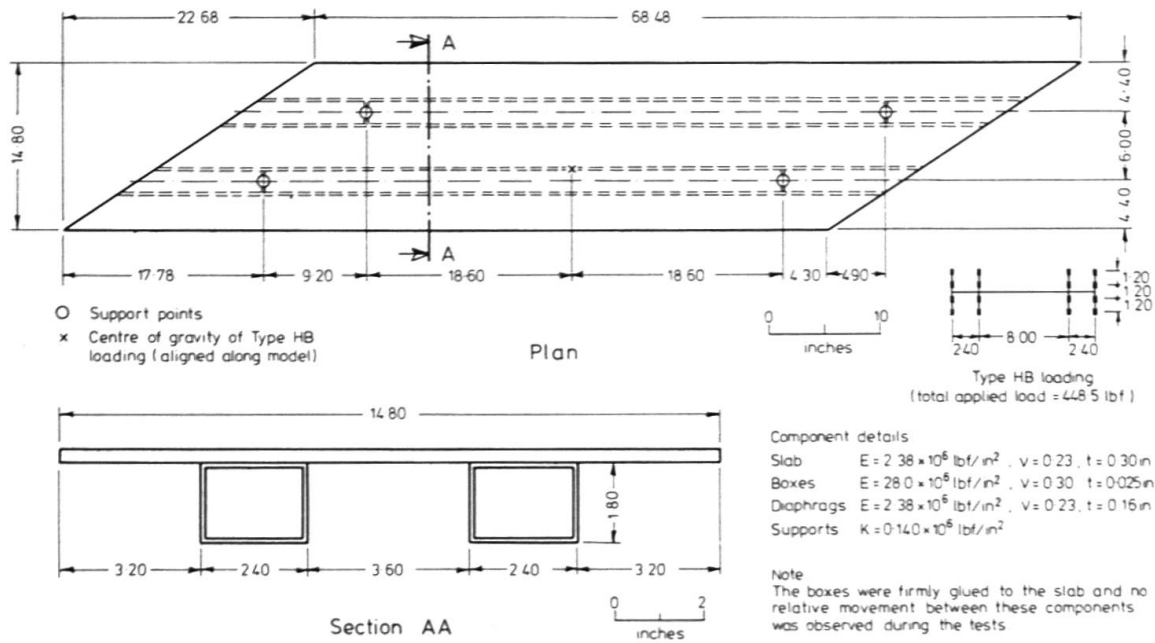
Component details

Slab $E = 2.38 \times 10^6$ lbf/in^2 , $v = 0.23$, $t = 0.30$ in
Boxes $E = 28.0 \times 10^6$ lbf/in^2 , $v = 0.30$, $t = 0.025$ in
Diaphrags $E = 2.38 \times 10^6$ lbf/in^2 , $v = 0.23$, $t = 0.16$ in
Supports $K = 0.140 \times 10^6$ lbf/in^2

Note
The boxes were firmly glued to the slab and no
relative movement between these components
was observed during the tests

Type HB loading
(total applied load = 448.5 lbf)

O   Support points
x   Centre of gravity of Type HB
    loading (aligned along model)

Plan

Section AA

Fig. 10   Composite twin cell box girder bridge model.
Details of model and loading

O   Support points

Plan

Section AA

Fig. 11   Composite twin cell box girder bridge model.
Finite element idealization

(a) Longitudinal outer surface stresses

(b) Transverse flexural slab stresses

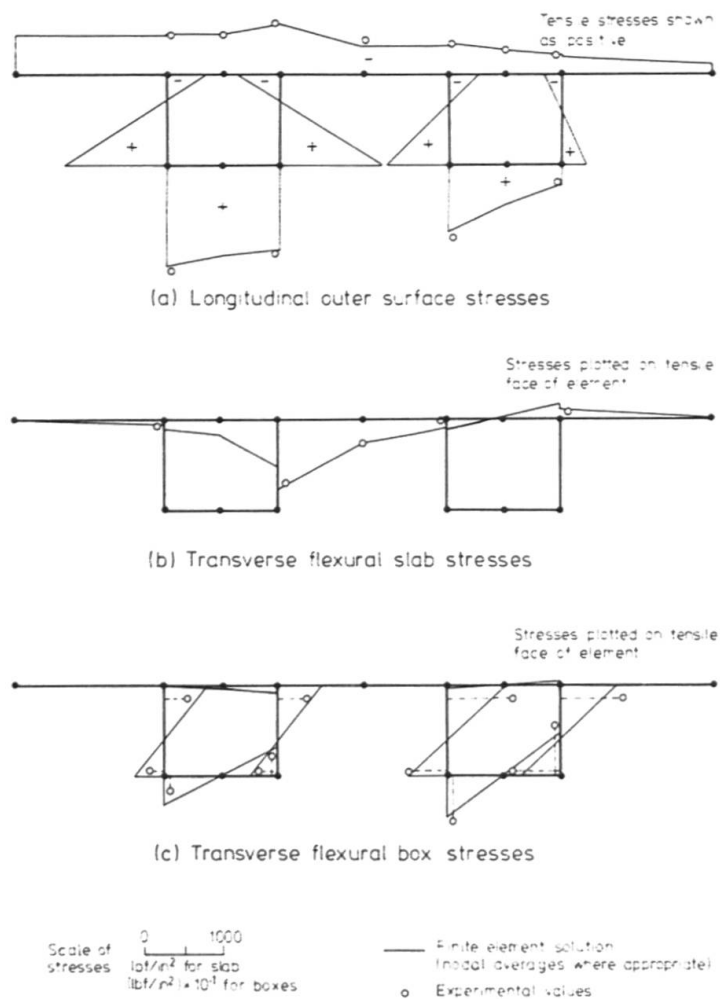(c) Transverse flexural box stresses

Fig 12 Composite twin cell box girder bridge model
Distribution of stresses at centre cross-section
for model under Type HB loading

4. PRACTICAL IMPLICATIONS AND CONCLUSIONS

An extensional-flexural element Q43 that is particularly suitable for use in
the analysis of box girder bridges has been developed. The efficiency of this
element has been compared with that of two elements Q23 and Q33, commonly
employed in the analysis of box girder bridges, by reference to the results of
three model tests. The comparisons showed that the element Q43 is much more
efficient than the element Q23 and slightly more efficient than the element Q33
in representing the overall behaviour of box girder bridges (the elements Q33
and Q43 can in fact give reliable results with as few as six and four mesh div-
isions, respectively, along each span and with one mesh division over the depth
of each web). The element Q43 has an additional advantage over the element Q33
in that it is particularly suitable for use in regions of high stress gradients,
such as those associated with the shear lag phenomenon [11].

Two triangular extensional-flexural elements T33 and T43 have been developed
for use with the elements Q33 and Q43, respectively. With the availability of
these elements it is possible to analyse a skewed box girder bridge using a
sub-division into triangular and rectangular elements. Such an idealization
gives more accurate results than an equivalent idealization employing only
parallelogrammic elements.

REFERENCES

1. Sawko, F.: Recent Developments in the Analysis of Steel Bridges using Electronic Computers. Proceedings of the British Constructional Steelwork Association Conference on Steel Bridges. Instn of Civ. Engrs, 1968.

2. Mehotra, B.L., Mufti, A.A., and Redwood, R.G.: Analysis of Three Dimensional Thin-walled Structures. J. struct. Div., Proc. Am Soc. Civ. Engrs, vol. 95, 1969, pp.2863-2872.

3. Zienkiewicz, O.C.: The Finite Element Method in Engineering Science. McGraw Hill, 1971.

4. Lim, P.T.K., Kilford, J.T., and Moffatt, K.R.: Finite Element Analysis of Curved Box Girder Bridges. Developments in Bridge Design and Construction (Proceedings of the International Conference at University College, Cardiff, 1971); edited by Rockey, K.C., Bannister, J.L., and Evans, H.R. Crosby Lockwood, 1972.

5. Sisodiya, R.G., Cheung, Y.K., and Ghali, A.: New Finite Elements with Application to Box Girder Bridges. Proc. Instn Civ. Engrs, supplement (XVII), 1972, pp.207-225.

6. Scordelis, A.C.: Analytical Solutions for Box Girder Bridges. Developments in Bridge Design and Construction (Proceedings of the International Conference at University College, Cardiff, 1971); edited by Rockey, K.C., Bannister, J.L., and Evans, H.R. Crosby Lockwood, 1972.

7. Lim, P.T.K. and Moffatt, K.R.: Finite Element Analysis of Curved Slab Bridges with Special Reference to Local Stresses. Developments in Bridge Design and Construction (Proceedings of the International Conference at University College, Cardiff, 1971); edited by Rockey, K.C., Bannister, J.L., and Evans, H.R. Crosby Lockwood, 1972.

8. Lim, P.T.K.: Elastic Analysis of Bridge Structures by the Finite Element Method. Ph.D. thesis, University of London, 1971.

9. Moffatt, K.R.: Finite Element Analysis of Box Girder Bridges. Ph.D. thesis, University of London, 1974.

10. Billington, C.J.: The Theoretical and Experimental Elastic Behaviour of Box Girder Bridges. Ph.D. thesis, University of London, 1974.

11. Moffatt, K.R., and Dowling, P.J.: Shear Lag in Steel Box Girder Bridges. Struct. Engr., vol. 53, 1975, pp.439-448.